Temperature control of fermentation bioreactor for ethanol production using IMC-PID controller

Munna Kumar, Durga Prasad, Balendu Shekher Giri, Ram Sharan Singh*

Chemical Engineering & Technology, Indian Institute of Technology (Banaras Hindu University), Varanasi 221005, India

A B S T R A C T

The state-space model is identified using the identification tool of MATLAB, and the best fit of 99% of measured and simulated data was obtained. Further, state-space model was converted to a transfer function model and finally simplified to an unstable second order time-delay transfer function model. Internal model control based proportional integral derivative (IMC-PID) controller design method was proposed for unstable second order time delay with RHP zero (USOPDT) and successfully tested to the nonlinear bioreactor process model. The temperature of the bioreactor was successfully controlled by proposed controller in both cases setpoint and disturbance change. The performance of the controller was evaluated in terms of IAE, ISE, ITAE and the corresponding values of 20.99, 49.02 and 292.50 were obtained respectively. Proposed method shows better closed-loop performance in terms of IAE and settling time than the other reported methods for temperature control of bioreactor.

1. Introduction

Biotechnology and biochemical process industry became an essential aspect of research in the last few decades due to its usefulness in the production of daily life use products like, medical and health sector products (medicines and vaccines), agro-based food like beer, wine etc. and in the treatment of industrial wastewater several biological processes occurred. The biochemical industry uses a living system or microorganisms to produce or manufacture the products to improve health standards and produces an alternative fuel [1,2]. The growth of microorganisms in the bioreactor depends on various process operating parameters such as inlet/outlet temperature and pH of the reactor. The literature shows that several conventional and advanced control techniques have been used to control the pH and temperature of the bioreactor. Nagy [3] developed the dynamic models of a bioreactor and used a feedforward artificial neural network (ANN) for temperature control of a continuous yeast fermentation process for ethanol production. The Linear Model Predictive Control (LMPC) technique, Proportional-Integral-Derivative (PID) controller and the neural network Model Predictive control schemes were used to control the reactor temperature, and the closed-loop

results of all methods were compared. A nonlinear model predictive control and model reduction technique with model parameter estimation was studied to control the anaerobic digestion process [4]. A fractional order IMC-PID (FOIMC-PID) and modified fractional order IMC-PID (MFOIMC-PID) were used for temperature control of the bioreactor in the fermentation process and further, a water cycle algorithm was used to optimize the designed controller parameters which lead to WMFOIMC-PID controller [1]. Takagi-Sugeno [5] and fuzzy-PI with split range control [6] were used to control the temperature of the bioreactor of the fermentation process. Pachauri et al. [7] suggested two degrees of freedom PID based inferential control for the temperature control of continuous bioreactor in a fermentation process.

Despite the development of the advanced control techniques, more than 95% of the process industrial control loop (chemical, biochemical, and pharmaceutical industries) uses PID type controller due to its simple structure, ease of implementation and robust nature [8–10]. Since the advanced control techniques such as Fuzzy logic, neural network, and model predictive control algorithms have a complicated mathematical approach and required more computation in order to control the process. These techniques also require replacement of controller to implement the control action whereas IMC-PID can be implemented on a PID controller and so no replacement of controller is required.

The conventional PID fails in several cases and shows poor performance due to the nonlinearity and instability of the process. To overcome these problems the internal model control based PID (IMC-PID) controller is developed which provides better

* Corresponding author.
  E-mail addresses: mkumar.rs.che14@itbhu.ac.in (M. Kumar),
dprasad.che@itbhu.ac.in (D. Prasad), balendushekher23@gmail.com (B.S. Giri),
rssingh.che@itbhu.ac.in (R.S. Singh).

closed-loop performance than the conventional PID design approach. It can be used to control both the stable and unstable process. A significant benefit over the conventional PID is that it has a single tuning parameter, which is easy to tune and implement to the real process. The IMC-PID controller for the different first and second order time delayed (FOPDT and SOPDT) stable, unstable and integrating process with or without having inverse response characteristics have been designed [11–15]. Kumar and Sree [16] has developed the IMC-PID controller for the integrating process and applied to the different single and double integrating process. They successfully implemented the proposed method to the nonlinear jacketed CSTR for temperature control. A nonlinear mathematical model of the reactor was linearized around operating conditions. The obtained higher order transfer function model was further approximated to the second order integrating process model. The controller parameters were obtained using the proposed method and applied to the process for the control purpose. An enhanced H_2 optimal IMC-PID was designed for different forms of the unstable integrating process and the method was successfully applied to the different linearized model of the non-linear process [17]. Babu et al. [18] studied the linearized unstable second order process model for the nonlinear process of crystallizer and jacketed CSTR and designed the PID controller using direct synthesis method to control the different unstable process models. Ram et al. [19] used an identification technique to obtained the unstable SOPDT model with a zero in the numerator and the optimization method was used to calculate the PI/PID parameters. The authors also proposed a method to find the initial guess.

It has been concluded from the literature that the several advanced control techniques (MPC, Fuzzy control, neural network etc.) and conventional control algorithm (PI, PID and IMC-PID) have been used for the temperature control of exothermic reaction carried out in CSTR and bioreactor. Therefore, the objectives of the present work are

(1) To develop the transfer function model of the bioreactor from the nonlinear mathematical model of the reactor.
(2) IMC-PID controller design for the second order unstable time delayed process model.
(3) Implementation of the proposed method to the nonlinear mathematical process model of the bioreactor for the temperature control.

2. Modeling of a continuous bioreactor

The mathematical model is developed by applying the law of physics i.e. mass and energy balances and it can be used by control engineer to implement the new control scheme without disturbing the real process. Some assumptions are necessary to make the model less complicated or simple in computation. The mathematical models of the process are simulated using the tool like MATLAB/SIMULINK and the dynamics of the models are obtained for further control application. A new control scheme can be developed with the help of these dynamics and applied to the model and finally to the real process without affecting the plant performance. Therefore, these models can recognize as an alternative to the real process, and the control designer can use it for the controller tuning, performance evaluation, optimizing the plant operation and handle the critical safety issue without disturbing the real process. Thus, the mathematical models are essential, efficient and powerful tools for implementing the new control schemes.

A continuous operating bioreactor in the fermentation process for the production of alcohol is considered here, i.e. the feed is added to the reactor and the product is continuously removed from the reactor. Therefore, the bioreactor can be assumed as a simple continuous stirred tank reactor (CSTR) in which different biological reactions are occurring. The biomass (*Saccharomyces cerevisiae*, yeast) and substrate (glucose) which feed the microorganisms for their growth, are the two main constituents of the bioreactor [20]. A stirrer is fitted in the middle of the reactor for the proper mixing of the biomass cells. Various products are obtained in a fermentation process. Ethanol is one of the most important products of the fermentation since it can be a substitute for petrol or it can be an alternative source of energy. The various assumptions of the bioreactor under consideration of the CSTR are:

- Perfect mixing
- Constant stirring speed
- pH of the bioreactor is constant
- the substrate feed flow and output flow from the reactor consists of the product are constant
- the input concentration of biomass and substrate are constant.

Fig. 1 shows the temperature control loop of the continuous bioreactor in which the temperature of the reactor is controlled by manipulating the jacket feed flow rate. The biomass production in the reactor is the main factor for the ethanol production rate and its high concentration and the production of biomass affected by the dilution rate (Fe/V). Therefore, the dilution rate should be low. The modified Monod equation according to the Michaelis–Menten developed by Aiba [21] gives the cell kinetics of the presented model.

$$\mu = \mu_o \frac{C_s}{K_s + C_s} e^{-K_1 C_p} \tag{1}$$

The mathematical models of the fermentation process for the production of alcohol have been developed in the literature and used by various researchers to achieve different control objectives by using different control algorithms. The mathematical models of the bioreactor for the production of ethanol have been developed and implemented for temperature control [1–3,5–7,20]. Therefore, these mathematical models of the bioreactor are also considered in the present study for temperature control. The IMC-PID has been designed for the unstable second order time delayed process and implemented to the bioreactor models. The mathematical models of the reactor are as follows:
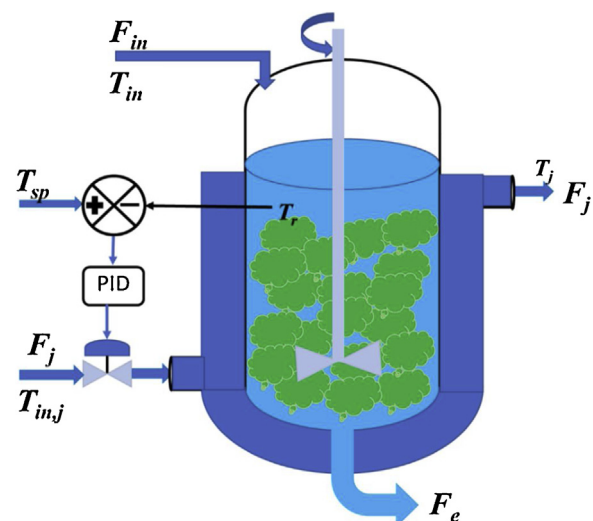

Fig. 1. Bioreactor temperature control loop.

Since the reactor is operating in continuous mode. Therefore, the total mass balance of the reactor is given by Eq. (2)

[rate of accumulation of total mass] = [input flow rate] – [output flow rate]

$$\frac{dv}{dt} = F_i - F_e \tag{2}$$

2.1. Mass balance of biomass

[rate of change of biomass (yeast) concentration] = [production of biomass in fermentation] – [biomass (yeast) leaving the reactor]

$$\frac{dC_x}{dt} = \mu_x C_x \frac{C_s}{K_s + C_s} e^{-K_p C_p} - \frac{F_e}{V} C_x \tag{3}$$

2.2. Mass balance for product ethanol

[rate of change of product (ethanol) concentration] = [production of ethanol in fermentation reaction] – [product (ethanol) leaving the reaction]

$$\frac{dC_p}{dt} = \mu_p C_x \frac{C_s}{K_{s1} + C_s} e^{-K_{p1} C_p} - \frac{F_e}{V} C_p \tag{4}$$

2.3. Mass balance for substrate (glucose)

[rate of change of substrate] = –[substrate consumed by biomass for growth] – [substrate consumed by biomass for ethanol production] + [glucose supplied by feed] – [glucose leaving the reaction]

$$\frac{dC_s}{dt} = -\frac{1}{R_{sx}} \mu_x C_x \frac{C_s e^{-K_p C_p}}{K_s + C_s} - \frac{1}{R_{sp}} \mu_p C_x \frac{C_s e^{-K_p C_p}}{K_{s1} + C_s} + \frac{F_{in}}{V} C_{s,in} - \frac{F_e}{V} C_s \tag{5}$$

2.4. Energy balance for reactor

For the growth of cells or ethanol the production in the fermentation process, the temperature of the bioreactor and jacket are an important parameter to consider. Since there is a certain temperature range for the growth of particular micro-organisms [22]. Hence, the mathematical model of the energy balance of the jacket and reactor must be included to improve the real-time performance of the process. The mathematical model of the energy balance for the jacket and the reactor are given as follows:

[Heat accumulated in reactor] = [Heat at inlet] – [Heat at outlet] + [Heat generated from reaction] – [Heat transferred to the jacketed]

$$\frac{dT_r}{dt} = \frac{F_{in}}{V}(T_{in} + 273) - \frac{F_e}{V}(T_r + 273) + \frac{r_{o_2}\Delta H_r}{32\rho_r C_{heat,r}} - \frac{K_T A_T (T_r - T_{in,j})}{V\rho_r C_{heat,r}} \tag{6}$$

2.5. Energy balance for jacket

[Heat accumulated in jacket] = [Heat at coolant inlet] + [Heat at coolant outlet]

$$\frac{dT_j}{dt} = \frac{F_j}{V_j}\left(T_{in,j} - T_j\right) + \frac{K_T A_T (T_r - T_j)}{V_j \rho_j C_{heat,j}} \tag{7}$$

2.6. Mass balance for dissolved oxygen concentration (C_{o_2})

[concentration of dissolved oxygen in the substrate during reaction] = [concentration of oxygen dissolved in inlet feed supplied to the reactor] – [consumption of oxygen in fermentation reactions]

$$\frac{dC_{o_2}}{dt} = K_L a\left(C_{o_2}^* - C_{o_2}\right) - r_{o_2} - \frac{F_e}{V} C_{o_2} \tag{8}$$

The growth of cells is affected by the concentration of dissolved oxygen (C_{o_2}) in the bioreactor of the fermentation process. The dissolved oxygen helps to grow the cells at a faster rate and increases cells density and ultimately increases oxygen consumption. Thus, the dissolved oxygen level decreases and therefore, required external oxygen supply to maintain the dissolved oxygen level [23]. The biomass overgrows in the presence of excess dissolved oxygen and ultimately the ethanol production rate decreases. Therefore, the dissolved oxygen should maintain at some optimum level so that the production rate of ethanol did not affect and achieved at the desired level of production rate [24]. The pH of the reactor is another important parameter which affects the operation of the bioprocess. The following models of dissolved oxygen concertation and pH of the bioreactor are implemented for the control purpose.

The liquid phase equilibrium concentration of oxygen is written as

$$C_{o_2}^* = \left(14.16 - 0.3943 T_r + 0.007714 T_r^2 - 0.0000646 T_r^3\right) 10^{-\sum H_i I_i} \tag{9}$$

The global effect of ionic strengths is given as follows

$$\sum H_i I_i = 0.5 H_{Na} \frac{m_{NaCl}}{M_{NaCl}} \frac{M_{Na}}{V} + 2 H_{Ca} \frac{m_{CaCO_3}}{M_{CaCO_3}} \frac{M_{Ca}}{V}$$
$$+ 2 H_{Mg} \frac{m_{MgCl_2}}{M_{MgCl_2}} \frac{M_{Mg}}{V} + 0.5 H_{Cl} \left(\frac{m_{NaCl}}{M_{NaCl}} + 2\frac{m_{MgCl_2}}{M_{MgCl_2}}\right) \frac{M_{Cl}}{V}$$
$$+ 2 H_{CO_3} \frac{m_{CaCO_3}}{M_{CaCO_3}} \frac{M_{CO_3}}{V} + 0.5 H_H 10^{-pH}$$
$$+ 0.5 H_{OH} 10^{-(14-pH)} \tag{10}$$

$$K_L a = K_L a_0 \cdot 1.024^{(T_r - 20)} \tag{11}$$

$$r_{o_2} = \mu_{o_2} \frac{1}{Y_{O_2}} C_x \frac{C_{O_2}}{K_{O_2} + C_{O_2}} \cdot 1000 \tag{12}$$

$$\mu_x = A_1 e^{\left[-\frac{E_{a1}}{R(T_r + 273)}\right]} - A_2 e^{\left[-\frac{E_{a2}}{R(T_r + 273)}\right]} \tag{13}$$

Eqs. (2)–(13) are simulated using MATLAB/SIMULINK and obtained the open-loop response curve of reactor temperature as shown in Fig. 3, by introducing the random value of the jacket flow rate. The open-loop response of the reactor temperature is identified by the Identification tool of the MATLAB and 99% best fit is obtained for measured and simulated data for 4th order of the state-space model. The bioreactor model parameters, steady-state operating parameters, and nomenclature are given in Appendix A, Appendix B, and Appendix C [1] and its open loop responses are shown in Fig. 2.

The state-space model of the plant is identified in the form of

$$\dot{X}(t) = A X(t) + B u(t) + K e(t) \tag{14}$$
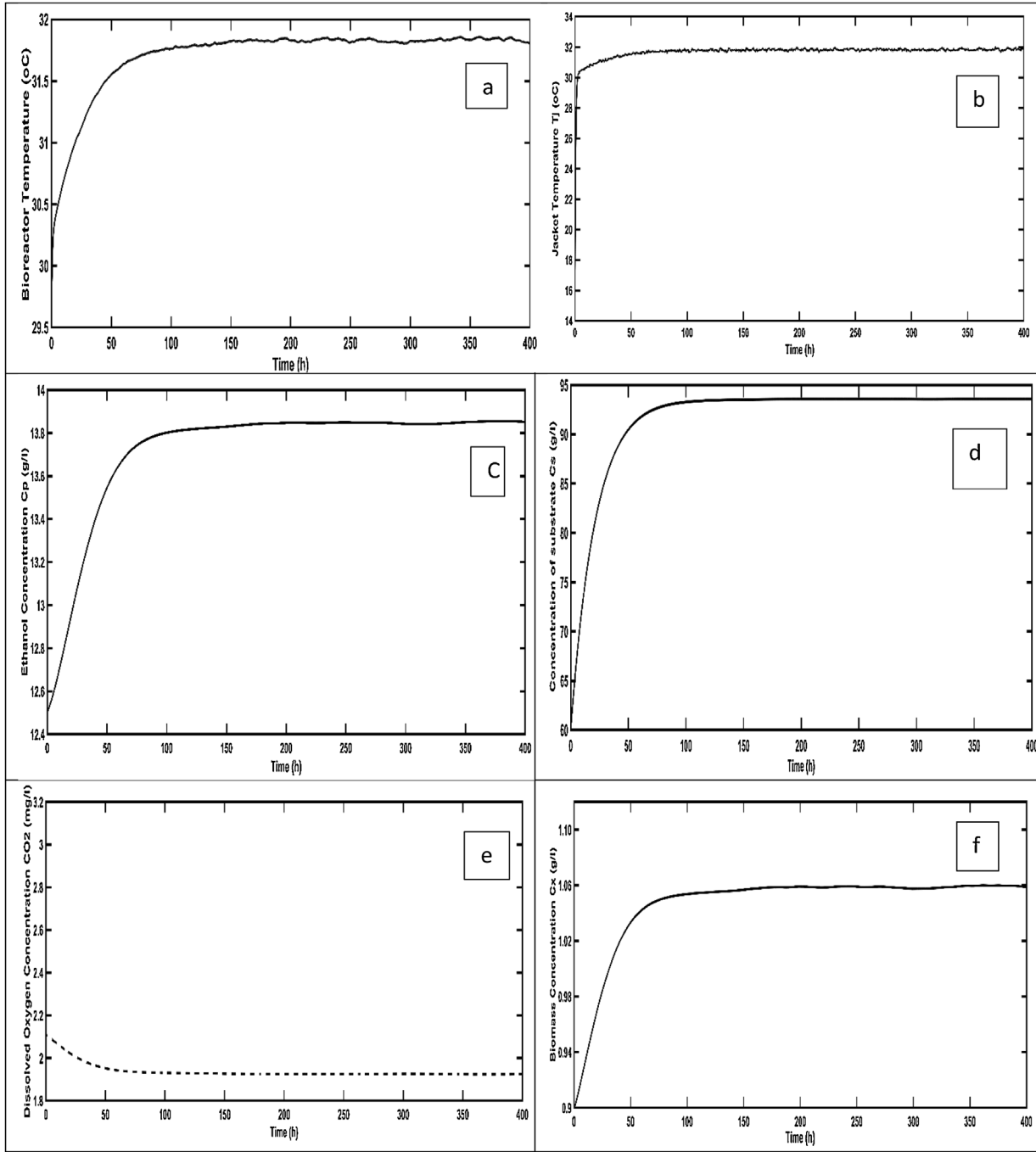
$$Y(t) = C X(t) + D u(t) + e(t) \tag{15}$$

Fig. 2. open-loop response of simulated bioreactor.

Where, X is the state variable, u denote the input variable Y is the output variable and $e(t)$ denote the disturbance. The Matrix A, B, C, D, and K are obtained by identification and model validation of process are as follows:

$$where, \quad A = \begin{bmatrix} -0.553 & -0.424 & -0.360 & -3.036 \\ -0.285 & -0.370 & -0.262 & 2.368 \\ -0.234 & -0.290 & -0.214 & -1.874 \\ 2.035 & 2.478 & 1.798 & -16.03 \end{bmatrix}, \quad B = \begin{bmatrix} -34.234 \\ -26.450 \\ -20.960 \\ 179.220 \end{bmatrix}$$

$$C = [138.595 \ 1654.6438 \ 989.568 \ 386.372], D = \begin{bmatrix} 1.667 \times 10^{-5} \end{bmatrix}, K = \begin{bmatrix} 0 \\ 0 \\ 0 \\ 0 \end{bmatrix}$$

Further, the state-space model is transformed into a transfer function model by introducing a unit step change into the inlet flow rate and the obtained transfer function model is given in Eq. (16)

$$G_p = \frac{-0.0032s^3 + 0.0048s^2 + 0.00363s + 4.018 \times 10^{-6}}{s^4 + 15.77s^3 + 2.68s^2 + 0.00857s + 9.75 \times 10^{-10}} \quad (16)$$

Further, after some simplification and neglecting the constant term in the numerator and denominator, since these values are lower as compared to other parameters and upon pole-zero cancellation of Eq. (16) can be written as follows and given in the Eq. (17).

$$G_p = \frac{0.555(s - 2.064)(1.8021s + 1)}{15.5982 \times 0.1685 \times 0.0033(0.0641s + 1)(5.9347s + 1)(303.03s + 1)} \quad (17)$$
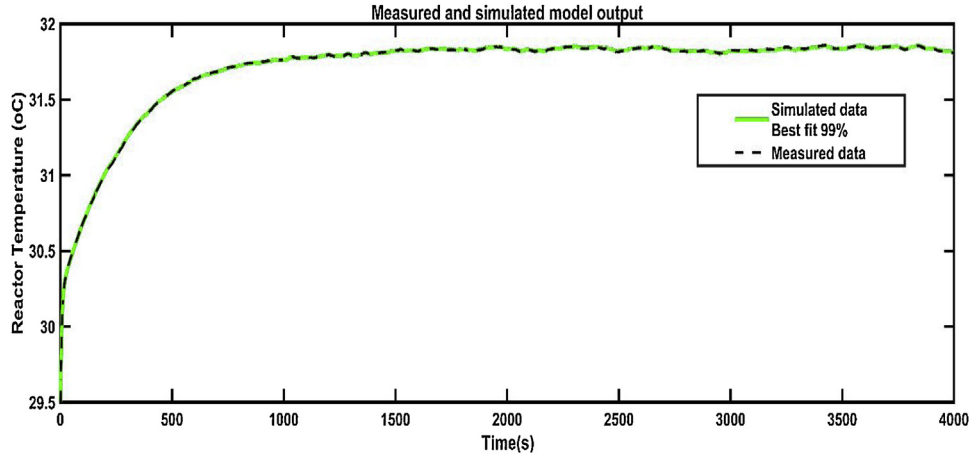
Fig. 3. Measured and simulated model output of the nonlinear process model.

Since one pole in the Eq. (17) is close to the origin, the behavior of the process model is nearly integrating. Therefore, the process model is simplified to the following form given Eq. (18)

$$G_p = \frac{-2.064 \times 0.211(-0.485s+1)(1.8021s+1)}{s(0.0641s+1)(5.9347s+1)} \quad (18)$$

The process model in Eq. (18) is 3rd order integrating process and it is difficult to calculate the PID parameters. Therefore, the process model is reduced to a second-order integrating process with time delayed by applying some reduction technique given by [25].

Skogestad [25] suggested that the inverse response behavior of the process is similar to the time delayed process since both have a deteriorating effect on the control action. Therefore, inverse response (RHP zero) term of the Eq. (19) can be approximated to time delayed term i.e.

$$(-0.485s+1) \approx e^{-0.485s} \quad (19)$$

By using Rule T2 given into Skogestad [25], the numerator and denominator term given in Eq. (21) can be approximated as

$$\frac{(1.8021s+1)}{(5.9347s+1)} \approx 0.303 \quad (20)$$

The integrating process has one pole at the origin due to which the process behavior similar to the unstable. Hence, using Eqs. (18)–(20) the final approximated transfer function model can be written as a required transfer function model was obtained as given in Eq. (20)

$$G_p = \frac{Tr(s)}{Fi(s)} = \frac{13.245}{(-100s+1)(0.0641s+1)} e^{-0.485s} \quad (21)$$

3. Control technique

Fig. 4 shows the closed-loop control scheme of (a) internal model control (IMC) and (b)simple feedback control. G_p indicates the process transfer function, G_m is the equivalent process model and the IMC controller is denoted by Q. $C(s)$ denotes to the feedback PI/PID controller. The different classes of unstable second order time delay (USOPDT) processes are available in the chemical and biochemical industries and which can be written by any one of the following model equations:

$$G_p = \frac{k_p e^{-\theta s}}{(\tau_1 s + 1)(\tau_2 s - 1)} \quad (22a)$$

$$G_p = \frac{k_p e^{-\theta s}}{(\tau_1 s - 1)(\tau_2 s - 1)} \quad (22b)$$

$$G_p = \frac{k_p e^{-\theta s}}{s(\tau s - 1)} \quad (22c)$$

$$G_p = \frac{k_p(1 \pm ps)e^{-\theta s}}{(\tau_1 s \pm 1)(\tau_2 s - 1)} \quad (22d)$$

The processes having both poles and zero in the right-hand plane (RHP) of the complex plane i.e RHP pole and zero (Eq. (22d)) are more difficult to control. Therefore, the process transfer function having at least one RHP pole and one RHP zero is considered for the controller design. The transfer function of the USOPDT could be in the form of Eqs. (22a)–(22c) then the designed method can also be applied to any one of these processes by converting to a standard form of the transfer function model.

For more general, the process model is considered in the form of

$$G_p = \frac{K_p(1-ps)e^{-\theta s}}{a_1 s^2 + a_2 s + 1} \quad (23)$$

Where $a_1 > 0$, $a_2 < 0$ and open-loop RHP poles of G_p may be real or complex.

According to the IMC principle, the IMC controller is designed as $Q = \tilde{Q}f(s)$

Where $f(s)$ is a low pass filter and which is used to make the controller internally stable and also to make the IMC controller Q proper and realizable. The filter selection also affect the robustness and performance of the controller.

Here, the IMC filter is selected from the literature as

$$f(s) = \frac{\beta_2 s^2 + \beta_1 s + 1}{(\lambda s + 1)^4} \quad (24)$$

For the designing of the IMC controller the process transfer function model is parameterized as

$$G_m = G_{m+}G_{m-}$$

where non-minimum phase part RHP zero and time delay is denoted by G_{m+} and the G_{m-} refers to the minimum phase part.
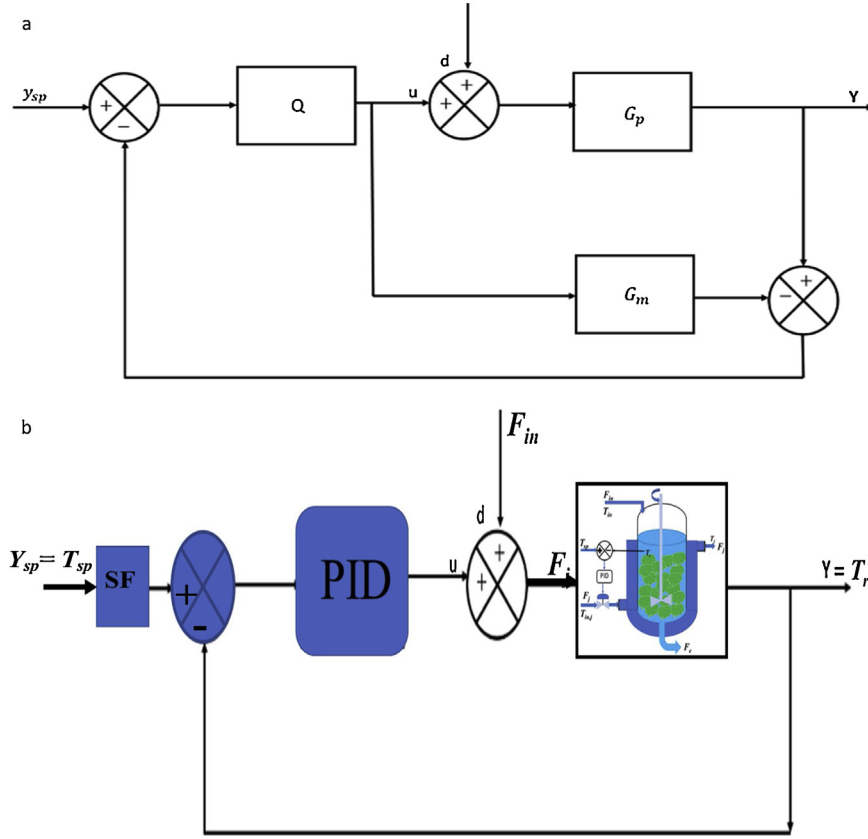
Fig. 4. (a) IMC control scheme; (b) Simple feedback control loop.

Therefore,

$$G_{m-} = \frac{K_p}{a_1 s^2 + a_2 s + 1} \text{ and } G_{m+} = (1 - ps)e^{-\theta s} \qquad (25)$$

So, IMC controller

$$Q = \tilde{Q}f(s) = \frac{a_1 s^2 + a_2 s + 1}{K_p} \times \frac{\beta_2 s^2 + \beta_1 s + 1}{(\lambda s + 1)^4} \qquad (26)$$

Moreover, the IMC control configuration is simplified to the following feedback control structure as

$$
\begin{aligned}
C(s) &= \frac{Q}{(1 - QG_p)} \\
&= \frac{(a_1 s^2 + a_2 s + 1)(\beta_2 s^2 + \beta_1 s + 1)}{K_p[(\lambda s + 1)^4 - (1 - ps)(\beta_2 s^2 + \beta_1 s + 1)e^{-\theta s}]}
\end{aligned} \qquad (27)
$$

Controller $C(s)$ obtained in the Eq. (27) is not in the standard form of the PID controller. Hence, Eq. (27) is simplified to the standard form of the PID with a lag filter in series. Using the Taylor series, the time delay term approximated as $e^{-\theta s} = 1 - \theta s$ in Eq. (27) and the controller can be written in the form of

$$C(s) = \frac{(a_1 s^2 + a_2 s + 1)(\beta_2 s^2 + \beta_1 s + 1)}{K_p[(\lambda s + 1)^4 - (1 - ps)(\beta_2 s^2 + \beta_1 s + 1)(1 - \theta s)]} \qquad (28)$$

Further, $C(s)$ is written into the following form

$$
\begin{aligned}
C(s) &= \frac{(a_1 s^2 + a_2 s + 1)(\beta_2 s^2 + \beta_1 s + 1)}{K_p(4\lambda - \beta_1 + \theta + p)s[x_1 s^3 + x_2 s^2 + x_3 s + 1]} \\
&= \frac{(a_1 s^2 + a_2 s + 1)(\beta_2 s^2 + \beta_1 s + 1)}{K_p hs[x_1 s^3 + x_2 s^2 + x_3 s + 1]}
\end{aligned} \qquad (29)
$$

Where,

$$h = (4\lambda - \beta_1 + \theta + p) \qquad (30a)$$

$$x_1 = \left(\lambda^4 - p\theta\beta_2\right) \qquad (30b)$$

$$x_2 = \left(4\lambda^3 - p\theta\beta_1 + \theta\beta_2 + p\beta_2\right) \qquad (30c)$$

$$x_3 = \left(6\lambda^2 - \beta_2 - \theta p + p\beta_1 + \theta\beta_1\right) \qquad (30d)$$

The denominator term of the Eq. (29), can be factorized as

$$x_1 s^3 + x_2 s^2 + x_3 s + 1 = (\gamma s + 1)(a_1 s^2 + a_2 s + 1) \qquad (31)$$

Upon equating the corresponding coefficients on both sides of Eq. (31), we get

$$x_1 = \gamma a_1 \qquad (32a)$$

$$x_2 = \gamma a_2 + a_1 \qquad (32b)$$

$$x_3 = \gamma + a_2 \qquad (32c)$$

By solving Eqs. (30) and (32), the coefficients β_1, β_2 and γ are caculated as

$$\beta_1 = \frac{y_4 z_1 - y_2 z_2}{y_1 y_4 - y_2 y_3} \qquad (33a)$$

$$\beta_2 = \frac{\beta_1 y_1 - z_1}{y_2} \tag{33b}$$

$$\gamma = \frac{x_1}{a_1} \tag{33c}$$

where,

$$y_1 = a_1 p\theta - a_1{}^2 \tag{34a}$$

$$y_2 = a_2 p\theta + a_1(p + \theta) \tag{34b}$$

$$y_3 = a_1(p + \theta) + a_1 a_2 \tag{34c}$$

$$y_4 = a_1 - p\theta \tag{34d}$$

$$z_1 = 4a_1\lambda^3 - a_2\lambda^4 - a_1{}^2(4\lambda + \theta + p) \tag{34e}$$

$$z_2 = \lambda^4 + a_1 a_2(4\lambda + \theta + p) - a_1(6\lambda^2 - p\theta) \tag{34f}$$

The final form of PID controller $G_c(s)$ is obtained as

$$C(s) = K_c\left(1 + \frac{1}{\tau_i s} + \tau_D s\right)\frac{1}{\alpha s + 1} \tag{35}$$

Where, $K_c = \frac{\beta_1}{K_p h}$, $\tau_i = \beta_1$, and $\tau_D = \frac{\beta_2}{\beta_1}$ and $\alpha = \gamma = \frac{x_1}{a_1}$ and λ is the tuning parameter. The tuning parameter λ is selected in such a way that the robust performance is obtained. There is no lead term in the designed controller filter, and α is small so this parameter does not have much effect on the performance of the designed controller.

The performance of the proposed method is compared in the terms of the various time integral error indices such as the integral of the squared error (ISE), integral of the absolute error (IAE), the integral of the time-weighted absolute error (ITAE). These performance indices can be written as following equations:

$$IAE = \int\limits_0^\infty ||e(t)||dt, \quad ISE = \int\limits_0^\infty e(t)^2 dt \text{ and } \quad ITAE = \int\limits_0^\infty t||e(t)||dt$$

Where, $e(t)$ is the error signal obtained by taking the difference of the set-point and output signal. The ISE error criteria are used for larger errors; the ITAE is applied in the case long time error appeared in the system, and the controller settings obtained by the IAE criterion minimizes the error lies between those of the ITAE and ISE criteria.

The maximum sensitivity measures the robustness of the controller and which is given as:

$$M_s = \max\left|\left|\frac{1}{1 + C(j\omega)G_p(j\omega)}\right|\right| \tag{36}$$

where, $C(j\omega)G_p(j\omega)$ denotes the open-loop transfer function, i.e., M_s is the inverse of the shortest distance from the Nyquist curve of the open-loop transfer function to the critical point $(-1, j0)$.

4. Results and discussion

The temperature is one of the essential parameters for the growth of microorganisms in the bioreactor as discussed in the literature. Various studies are available in the literature in which different advanced control algorithms have been developed for the reactor temperature control. Since the bioreactor operates in a narrow range of temperature during the fermentation process, an effective control mechanism is required for the tight control of reactor temperature for the optimal growth of microorganisms. Thus, in the present study, IMC-PID controller has been proposed for the temperature control of the reactor.

The controller parameters are calculated for the transfer function model of bioreactor obtained in Eq. (22) using proposed method of IMC-PID design and which are listed in Table 1. The reactor is operated in continuous mode and it is assumed that the substrate input and output flow rate are same $F_{in} = F_e$. Input substrate feed flow rate F_{in}, substrate feed temperature T_{in}, and the input cooling liquid temperature $T_{in,j}$ are also assumed to be constant during the simulation. It is also assumed that a constant substrate feed flow rate is supplied to the bioreactor. The

Table 1
PID parameters and performance of the controller for the process model.

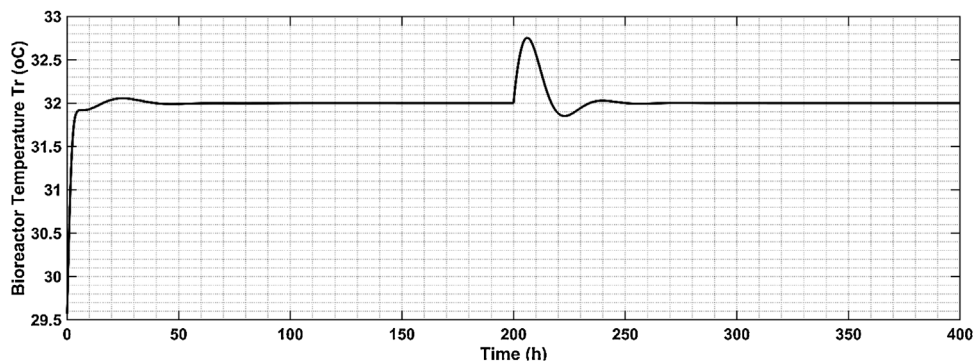| Model	Tuning parameter	PID parameters			Robustness	Set-point Change			Disturbance Change		
	λ	K_c	τ_I	τ_D	M_s	IAE	ITAE	ISE	IAE	ITAE	ISE
USOPDT	0.8	9.56	3.66	2.34	5.173	20.99	49.02	292.5	46.73	299.2	436.2

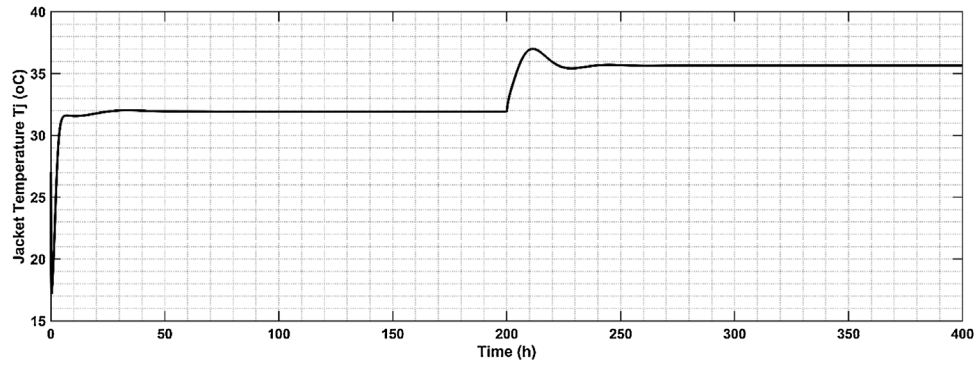**Fig. 5.** Bioreactor temperature control for set-point and disturbance change.

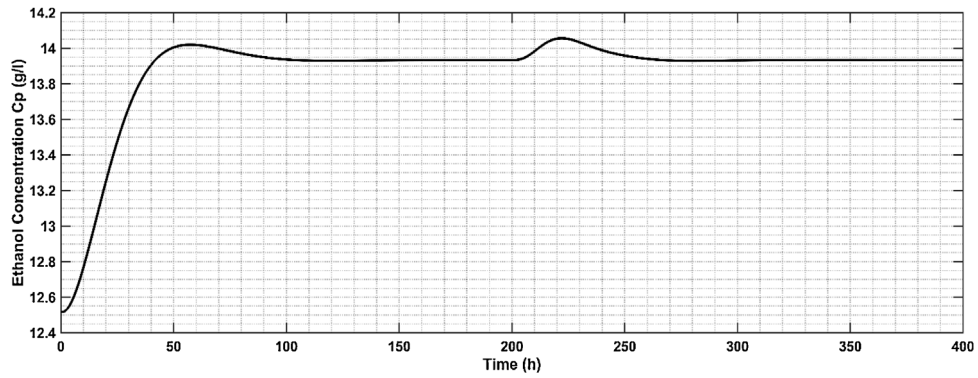**Fig. 6.** Jacket temperature control for set-point and disturbance change.

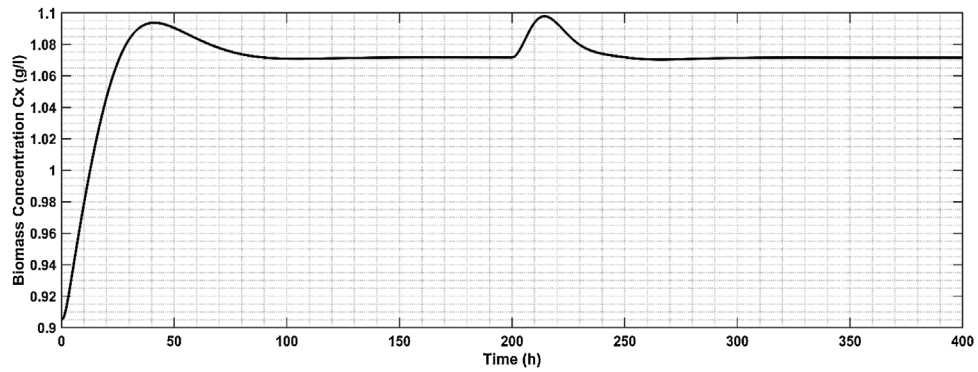**Fig. 7.** Concentration of ethanol corresponding to controlled reactor temperature.

Fig. 8. Concentration of substrate corresponding to controlled reactor temperature.
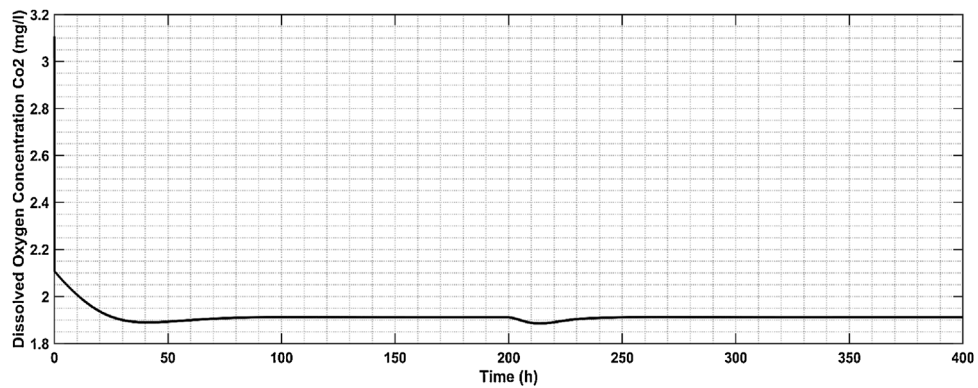

Fig. 9. Concentration of dissolved oxygen corresponding to controlled reactor temperature.

temperature of the bioreactor T_r is the controlled variable and the input flow rate F_j to the jacket is the manipulated variable. The temperature of the bioreactor is controlled by using the PID controller as the control structure shown in Fig. 4(b) by manipulating the inlet flow rate F_j of the jacket. It is noted that the obtained PID controller is implemented to the nonlinear model of the process by taking reactor temperature T_r as the controlled variable and the input flow rate F_j to the jacket is the manipulated variable. The simulated closed-loop response for the servo as well as regulatory problems for reactor temperature is shown in Fig. 5. The disturbance is introduced at 200 h by giving a unit step change to the substrate inlet flow rate F_{in}. The temperature of the reactor T_r achieved set-point (32 °C) quickly and took about 9 h to reach the set-point in case of servo problem and around 20 h in case of the regulatory problem. A first-order set-point filter of $f = 1/(0.9\lambda s + 1)$ is used to remove the undesirable overshoot. The performance of the controller is evaluated in terms of the various time integral error indices like integral absolute error (IAE), integral square error (ISE) and integral time absolute error (ITAE) and listed in Table 1. Pachauri et al. [1] applied three different control methods as water cycle optimization modified fractional order IMC-PID (WMFOIMC-PID), water cycle optimization fractional order PID (WFOPID) and water cycle optimization PID controllers and obtained IAE values of 43.68, 102.34 and 158.23 respectively for set point tracking. However, in the present method IAE value of 20.99 is obtained in case of set point change, which is lower than all of the methods suggested by Pachauri et al. [1]. Hernández et al. [5] used the Takagi-Sugeno modeling technique for the modeling of the nonlinear bioreactor and temperature control. The proposed method shows a lower settling time than this method and the 4% of overshoot obtained which is slightly greater. A fuzzy split range control system was applied to the same problem of the present study of a fermentation process. The ITAE value in case of SRI, SRII, SRIII for conventional PI controller are 2913, 2815, 3015, in case of PID controller 1400, 1382 and 1442, for Fuzzy PI 4295, 4071 and 4300 and in case of Fuzzy PID controller 10120, 9590 and 10,580 respectively were obtained and which are much greater than the present method. Figs. 5 and 6 show bioreactor temperature T_r and jacket liquid temperature T_j respectively for set-point change as well as disturbance change. In set point change the reactor temperature T_r attain quickly to set point and the jacket temperature T_j also attained nearly equal to the T_r and similar results were obtained in [7]. But, in case of unit disturbance change i.e., by increasing the inlet flow rate F_{in} of the substrate, the reactor temperature took about 30 h to reach set-point and the jacket temperature T_j achieved a greater value than the T_r it concludes that the jacket removes more heat. Figs. 7–9 show the behavior of the ethanol concentration, biomass concentration and dissolved oxygen corresponding to the controlled reactor temperature T_r.

5. Conclusions

In the present study, the open loop response of bioreactor temperature in the fermentation process for ethanol production was recorded and then best fitted into state space model. Finally converted into the form of unstable second-order time-delay system. IMC-PID was proposed for unstable second order time delay with RHP zero (USOPDT) and successfully tested to control bioreactor temperature in the fermentation process for ethanol production. Performance of the proposed IMC-PID controller was evaluated for set point and load change in the temperature of the bioreactor. Temperature of the bioreactor was successfully controlled by proposed method for setpoint and load change which was evident from acceptable values of time integral error indices. The value of IAE in the present study was found better than values obtained by previous researchers whereas the values of

other two indices (ISE and ITAE) were also calculated. The study demonstrated that the proposed technique can effectively be used to control bioreactor's temperature.

Conflict of interest

All authors are mutually agreed for the submission of the manuscript to the Biotechnology Reports journal for possible publication. Therefore, there is no conflict of interest.

Acknowledgments

Appendix A. Bioreactor model parameters

$A_1 = 9.5 \times 10^8$	$H_{Na} = -0.55$	$\rho_r = 1080$ g L^{-1}
$A_2 = 2.55 \times 10^{33}$	$K_L a_0 = 38$ h^{-1}	$m_{NaCl} = 500$ g
$A_T = 1$ m^2	$K_{O_2} = 8.886$ mg L^{-1}	$m_{CaCO_3} = 100$ g
$C_{heat,ag} = 4.18$ J g^{-1} K^{-1}	$K_P = 0.139$ g L^{-1}	$m_{MgCl_2} = 100$ g
$C_{heat,r} = 4.18$ J g^{-1} K^{-1}	$K_{p1} = 0.07$ g L^{-1}	$R = 8.31$ J mol^{-1} K^{-1}
$E_{a1} = 55,000$ J mol^{-1}	$K_S = 1.03$ g L^{-1}	$M_{Na} = 23$ g mol^{-1}
$E_{a2} = 22,000$ J mol^{-1}	$K_{S1} = 1.68$ g L^{-1}	$M_{Ca} = 40$ g mol^{-1}
$H_{OH} = 0.941$	$K_T = 3.6 \times 10^5$ J h^{-1} m^{-2} K^{-1}	$M_{Mg} = 24$ g mol^{-1}
$H_H = -0.774$	$R_{SP} = 0.435$	$M_{Cl} = 35.5$ g mol^{-1}
$H_{CO_3} = 0.485$	$R_{Sx} = 0.607$	$M_{CO_3} = 60$ g mol^{-1}
$H_{Cl} = 0.844$	$Y_{O_2} = 0.970$ mg mg^{-1}	$\mu_P = 1.79$ h^{-1}
$H_{Mg} = -0.314$	$\Delta Hr = 518$ kJ mol^{-1} O$_2$	$\rho_u = 1000$ g L^{-1}
$H_{Ca} = -0.303$	$\mu_{O_2} = 0.5$ h^{-1}	

Appendix B. steady-state operating parameters

Parameter	Description	Values
F_i	Input Flow	51 L h^{-1}
F_e	Output Flow	51 L h^{-1}
T_{in}	Inlet flow temperature	25 °C
T_e	Output Flow temperature	25 °C
$T_{in,j}$	Temperature of input Cooling agent	15 °C
$C_{s,in}$	Concentration of Glucose input Flow	60 g L^{-1}
$K_L a$	Mass Transfer Coefficient for oxygen	$38(1024)^{T_r-20}$
V	Total volume of the reaction medium	1000 L
V_j	Volume of the jacket	50 L
pH	Potential of hydrogen	6
F_j	Flow rate of cooling agent	18 L h^{-1}

Appendix C. Nomenclature

A_1, A_2	Exponential factors in Arrhenius equation
A_T	Heat transfer area (m^2)
$C_{heat,j}$	Heat capacity of cooling agent
$C_{heat,r}$	Heat capacity of the fermentation medium
E_{a1}, E_{a2}	Activation energy
CE_i	Control effort for valve i
C_{O_2}	Oxygen concentration in the liquid phase (mg L^{-1})
$C_{O_2}^*$	Equilibrium concentration of oxygen in the liquid phase (mg L^{-1})
$C_{O_2,0}^*$	Equilibrium concentration of oxygen in distilled water (mg L^{-1})
C_P	Ethanol concentration (g L^{-1})
C_S	Glucose concentration (g L^{-1})
$C_{S,in}$	Glucose concentration in the feed stream (g L^{-1})

C_x	Biomass concentration (g L^{-1})
e	Controlled variable error (ºC)
F_e	Bioreactor downstream flow (L h^{-1})
F_h	Hot utility flow (L h^{-1})
F_{in}	Bioreactor feed flow (L h^{-1})
H	Specific ionic constant
I	Ionic strength
$K_L a$	Product of the mass-transfer coefficient for oxygen and gas-phase specific area $\left(\text{h}^{-1}\right)$
K_{O_2}	Constant for oxygen consumption mg L^{-1}
K_P	Constant of growth inhibition by ethanol (g L^{-1})
K_{P1}	Constant of fermentation inhibition by ethanol (g L^{-1})
K_S	Constant in the substrate term for growth (g L^{-1})
K_{S1}	Constant in the substrate term for ethanol production (g L^{-1})
K_T	Heat transfer coefficient $(\text{J h}^{-1}\text{m}^{-2}\text{K}^{-1})$
m	Quantity of inorganic salt (g)
M	Molecular/atomic mass (g mol^{-1})
r_{O_2}	Oxygen uptake rate $\text{mg L}^{-1} \quad \text{h}^{-1}$
R	Universal gas constant $(\text{J mol}^{-1} \quad \text{K}^{-1})$
R_{SP}	Ratio of ethanol produced per glucose consumed for fermentation
R_{SX}	Ratio of cell produced per glucose consumed for growth
T	Time (h)
T_{in}	Temperature of the substrate flow entering to the bioreactor (ºC)
T_j	Jacket temperature (°C)
T_r	Temperature in the bioreactor (°C)
$u_{k,i}$	Control signal to valve i at moment k (mA)
V	Volume of the bioreactor (L)
V_j	Volume of the jacket (L)
Y_{O_2}	The amount of oxygen consumed per unit biomass produced (mg/mg)
ΔH_r	Reaction heat of fermentation $(\text{KJ} \quad \text{mol}^{-1}\, O_2 \text{ Consumed})$
Δu_i	Normalized control signal variation
μ_{O_2}	Maximum specific oxygen consumption rate (h^{-1})
μ_P	Maximum specific fermentation rate (h^{-1})
μ_x	Maximum specific growth rate (h^{-1})
ρ_j	Density of jacket liquid (g L^{-1})
ρ_r	Density of the fermentation medium (g L^{-1})

References

[1] N. Pachauri, A. Rani, V. Singh, Bioreactor temperature control using modified fractional order IMC-PID for ethanol production, Chem. Eng. Res. Des. 122 (2017) 97–112.

[2] U. Imtiaz, S.S. Jamuar, J. Sahu, P. Ganesan, Bioreactor profile control by a nonlinear autoregressive moving average neuro and two degree of freedom PID controllers, J. Process Control 24 (11) (2014) 1761–1777.

[3] Z.K. Nagy, Model-based control of a yeast fermentation bioreactor using optimally designed artificial neural networks, Chem. Eng. J. 127 (1–3) (2007) 95–109.

[4] M. Ławryńczuk, Modelling and nonlinear predictive control of a yeast fermentation biochemical reactor using neural networks, Chem. Eng. J. 145 (2) (2008) 290–307.

[5] A. Flores-Hernández, J. Reyes-Reyes, C. Astorga-Zaragoza, G. Osorio-Gordillo, C. García-Beltrán, Temperature control of an alcoholic fermentation process through the Takagi–Sugeno modeling, Chem. Eng. Res. Des. 140 (2018) 320–330.

[6] R.R. Fonseca, J.E. Schmitz, A.M.F. Fileti, F.V. da Silva, A fuzzy–split range control system applied to a fermentation process, Bioresour. Technol. 142 (2013) 475–482.

[7] N. Pachauri, V. Singh, A. Rani, Two degree of freedom PID based inferential control of continuous bioreactor for ethanol production, ISA Trans. 68 (2017) 235–250.

[8] K.J. Åström, T. Hägglund, PID controllers: theory, design, and tuning, Instrum. Soc. Am. Res. (Triangle Park, NC) 10 (1995).

[9] K.J. Åström, T. Hägglund, The future of PID control, Control Eng. Pract. 9 (11) (2001) 1163–1175.

[10] K.J. Åström, T. Hägglund, Revisiting the Ziegler–Nichols step response method for PID control, J. Process Control 14 (6) (2004) 635–650.

[11] Q. Wang, C. Lu, W. Pan, IMC PID controller tuning for stable and unstable processes with time delay, Chem. Eng. Res. Des. 105 (2016) 120–129.

[12] M. Shamsuzzoha, A unified approach for proportional-integral-derivative controller design for time delay processes, Korean J. Chem. Eng. 32 (4) (2015) 583–596.

[13] J. Lee, W. Cho, T.F. Edgar, Simple analytic PID controller tuning rules revisited, Ind. Eng. Chem. Res. 53 (13) (2013) 5038–5047.

[14] M. Shamsuzzoha, M. Lee, IMC−PID controller design for improved disturbance rejection of time-delayed processes, Ind. Eng. Chem. Res. 46 (7) (2007) 2077–2091.

[15] M. Shamsuzzoha, M. Lee, Design of advanced PID controller for enhanced disturbance rejection of second-order processes with time delay, AlChE J. 54 (6) (2008) 1526–1536.

[16] D.S. Kumar, R.P. Sree, Tuning of IMC based PID controllers for integrating systems with time delay, ISA Trans. 63 (2016) 242–255.

[17] K.G. Begum, A.S. Rao, T. Radhakrishnan, Enhanced IMC based PID controller design for non-minimum phase (NMP) integrating processes with time delays, ISA Trans. 68 (2017) 223–234.

[18] D. Chanti Babu, D. Santosh Kumar, R. Padma Sree, Tuning of PID controllers for unstable systems using direct synthesis method, Indian Chem. Eng. 59 (3) (2017) 215–241.

[19] V.D. Ram, A. Karlmarx, M. Chidambaram, Identification of unstable second-order transfer function model with a zero by optimization method, Indian Chem. Eng. 58 (1) (2016) 29–39.

[20] S. Ramaswamy, T. Cutright, H. Qammar, Control of a continuous bioreactor using model predictive control, Process Biochem. 40 (8) (2005) 2763–2770.

[21] S. Aiba, M. Shoda, M. Nagatani, Kinetics of product inhibition in alcohol fermentation, Biotechnol. Bioeng. 10 (6) (1968) 845–864.

[22] M.L. Shuler, F. Kargi, Bioprocess Engineering: Basic Concepts, 2nd ed., (2002) Upper Saddle.

[23] P. Tervasmäki, M. Latva-Kokko, S. Taskila, J. Tanskanen, Effect of oxygen transfer on yeast growth—growth kinetic and reactor model to estimate scale-up effects in bioreactors, Food Bioprod. Process. 111 (2018) 129–140.

[24] T.W. Nagodawithana, C. Castellano, K.H. Steinkraus, Effect of dissolved oxygen, temperature, initial cell count, and sugar concentration on the viability of Saccharomyces cerevisiae in rapid fermentations, Appl. Microbiol. 28 (3) (1974) 383–391.

[25] S. Skogestad, Simple analytic rules for model reduction and PID controller tuning, J. Process Control 13 (4) (2003) 291–309.